

# Invalidation of fMRI Experiments Secondary to Neurovascular Uncoupling in Patients With Cerebrovascular Disease

Andrea E. Para, MD,<sup>1,2</sup> Kevin Sam, PhD,<sup>2</sup> Julien Poublanc, MSc,<sup>2</sup>  
Joseph A. Fisher, MD,<sup>3</sup> Adrian P. Crawley, PhD,<sup>2,4</sup> and David J. Mikulis, MD<sup>2,4\*</sup>

**Purpose:** Blood oxygen level-dependent (BOLD) functional magnetic resonance imaging (fMRI) is a technique used to infer neuronal activity from the observed changes in blood flow. Cerebrovascular reactivity (CVR) is the ability of arterioles to increase blood flow in response to vasodilatory stimulus. We hypothesize that in areas of disease where there is exhausted vascular reserve and impaired CVR there will be diminished blood flow response following neuronal activation, and that these areas would appear as false-negative tests on BOLD fMRI.

**Materials and Methods:** Patients with steno-occlusive disease and unilateral hemodynamic impairment received a standardized hypercapnic stimuli while being imaged with BOLD fMRI to generate CVR maps. These were compared to traditional BOLD fMRI maps of neuronal activation in the motor cortex in response to a motor task.

**Results:** Neuronal activation from the motor task was found to be linearly correlated with CVR ( $n = 11$  patients,  $R = 0.82$ ). Regions with positive (normal) CVR showed positive activation on BOLD fMRI, while regions with negative CVR had attenuated neuronal activation on BOLD fMRI.

**Conclusion:** In areas with cerebrovascular disease where CVR is impaired, there is uncoupling of neuronal activation and blood flow that confounds traditional BOLD fMRI. CVR mapping is a noninvasive MRI-based imaging technique that can provide information about the vascular reactivity of the brain that is important to consider when interpreting traditional BOLD fMRI studies.

**Level of Evidence:** 2

**Technical Efficacy:** Stage 3

J. MAGN. RESON. IMAGING 2017;46:1448–1455.

Cerebral blood flow (CBF) is tightly regulated not only to maintain stable flow conditions during fluctuations in blood pressure (autoregulation) but also to supply additional flow in support of increased metabolic activity associated with neuronal signaling. The latter relationship, termed neurovascular coupling, is mediated through signaling mechanisms originating from neurons and glial cells targeted to the vascular endothelium and smooth muscle. The final effector for both autoregulation and neurovascular coupling is the tone of arteriolar smooth muscle that controls blood vessel diameter and therefore vascular resistance. Smooth muscle tone can be affected by numerous agents including blood

pressure, the partial pressure of oxygen and carbon dioxide ( $PO_2$  and  $PCO_2$ ), drugs (such as nicotine, ethanol, and caffeine), as well as mediators derived from neural signaling.<sup>1</sup>

Cerebrovascular reactivity (CVR) is the ability of arterioles to increase blood flow in response to a vasodilatory stimulus such as a change in blood pressure or a change in  $PCO_2$ . The full range of this response is termed cerebrovascular reserve. If a mild or moderate proximal vascular resistance were to develop from, for example, a large vessel arterial stenosis, a compensatory vasodilatory response would occur, consuming some of the existing vascular reserve and CVR would be reduced. However, for severe stenoses or occlusions or under conditions where cerebral tissue is compressed

View this article online at [wileyonlinelibrary.com](http://wileyonlinelibrary.com). DOI: 10.1002/jmri.25639

Received Sep 30, 2016, Accepted for publication Jan 3, 2017.

\*Address reprint requests to: D.J.M., Toronto Western Hospital, McLaughlin Pavilion, 3rd Floor, Room 431, 399 Bathurst St., Toronto, ON, Canada M5T 2S8.  
E-mail: [mikulis@mac.com](mailto:mikulis@mac.com)

From the <sup>1</sup>Department of Medical Imaging, University of Western Ontario, London, Canada; <sup>2</sup>Division of Neuroradiology, Joint Department of Medical Imaging, University Health Network, Toronto, Canada; <sup>3</sup>Department of Anesthesiology, University Health Network and University of Toronto, Toronto, Canada; and <sup>4</sup>Department of Medical Imaging, University of Toronto, Toronto, Canada

Additional Supporting Information may be found in the online version of this article

**TABLE 1. Patient Demographics**

Subject	Age	Sex	Side of CVR impairment	Etiology
1	47	M	R	R-MCA occlusion, L-MCA stenosis
2	80	M	B	R+L ICA occlusion, B-MMD, L-ECIC bypass
3	34	F	B	B-MMD, R-ECIC bypass
4	22	M	R	R-MMD, R-ECIC bypass
5	57	M	L	B-MMD, R+L ICA stenosis, L-ECIC bypass
6	67	F	L	L-ICA and L-MCA occlusion
7	37	F	R	R-MMD, R-ECIC bypass
8	18	F	R	R-MMD, R-ECIC bypass
9	42	F	L	B-MMD, L-ECIC bypass
10	74	F	R	R+L ICA stenosis, L-CEA
11	56	M	R	R-ICA occlusion, R-CEA, R-ECIC bypass

B = bilateral; CEA = carotid endarterectomy; ECIC = extracranial-intracranial; EPI = echo-planar imaging; ICA = internal carotid artery; MCA = middle cerebral artery; MMD = moyamoya disease; L = left-sided; R = right-sided; ROI = region of interest (ROI was drawn over the hand representation of the motor cortex on T1-weighted images).

or edematous secondary to neoplastic disease, vasodilatation may already be maximal simply to preserve resting blood flow. Under these circumstances vascular reserve is fully consumed and further vasodilatation, for example, in response to neural activity, is not possible. In fact, severe cases can result in “steal” physiology where there is a paradoxical decrease in blood flow in response to a vasodilatory stimulus caused by diversion of flow away from vascular territories that are fully vasodilated (where there is fixed flow resistance) to those vascular beds that can still vasodilate (where flow resistance can decrease).<sup>2</sup>

Blood oxygen level-dependent (BOLD) functional magnetic resonance imaging (fMRI) has been used for roughly 25 years to identify neural activity based on the principle of detecting increased capillary and venular oxygenation associated with increased neuronal activity. This produces an increase in BOLD signal that is dependent on delivery of more oxygen than is consumed by neural activation. In fact, in one of the most referenced studies that has examined this relationship, blood flow increases of 45% with increases in oxygen consumption of only 16% were observed.<sup>3</sup> A key question is what would happen to the BOLD signal in tissue where vascular reserve is fully consumed and vasodilation is not possible? We hypothesize that in these areas neurons may be active, but if the surrounding vasculature is unable to respond appropriately, the level of activation inferred from the BOLD signal will likely be incorrect (type II error). This may lead to erroneous mapping of the brain network being investigated, with significant implications for research and clinical applications of BOLD fMRI in these subjects.

The aim of this study was to demonstrate that CVR mapping<sup>4</sup> is important to consider when interpreting

BOLD fMRI studies in areas of cerebrovascular disease and steal physiology.

## Materials and Methods

### Ethics and Consent

Ethics approval was obtained from the Institutional Ethics Review Board. The protocol was reviewed with each subject and informed consent was obtained from each patient.

### Patient Selection

Eleven patients with a history of steno-occlusive disease who were recruited for CVR studies as part of an ongoing prospectively managed database (Table 1) performed an additional motor task during BOLD imaging.

### Functional Scans

All images were acquired on a 3.0T MRI scanner (Signa HDX platform, GE Healthcare, Milwaukee, WI). Both the CVR and motor task experiments were imaged using a BOLD pulse sequence with the following parameters: repetition time (TR) = 2000 msec, echo time (TE) = 30 msec, flip angle = 85°, 28 slices, slice thickness = 5 mm, 64 × 64 matrix size, field of view (FOV) = 200 mm, and an echo planar imaging readout.

### Anatomical Scan

In addition, high-resolution  $T_1$ -weighted anatomical images were acquired for coregistration and spatial normalization purposes consisting of an inversion recovery-prepared spoiled gradient-recalled sequence with the following parameters: flip angle = 20°, TI/TE/TR = 300/5/11.5 msec, 146 slices of 1 mm thickness and a 256 × 256 matrix size with 200 mm FOV.

### **CVR and Control of PCO<sub>2</sub>**

A customized gas blender with an airtight sequential rebreathing mask (RespirAct; Thornhill Research Institute, Toronto, Canada) was used to apply two pseudo-square wave changes in end-tidal CO<sub>2</sub> (PETCO<sub>2</sub>) while maintaining iso-oxic end-tidal O<sub>2</sub> levels.<sup>5–7</sup> Previously, in development of the rebreathing system end-tidal CO<sub>2</sub> measurements were compared with arterial blood gas measurements of CO<sub>2</sub> and it was found that the sequential gas delivery system ensured that end-tidal CO<sub>2</sub> was within  $\pm 2$  mmHg of the arterial CO<sub>2</sub>.<sup>8</sup> The gas blender delivers set mixtures of O<sub>2</sub>, N<sub>2</sub>, and CO<sub>2</sub> to the mask to obtain targeted elevations of end-tidal CO<sub>2</sub> to 10 mmHg above baseline ( $\sim 40$  mmHg, measured in each patient individually) while maintaining end-tidal O<sub>2</sub> levels constant at 100 mmHg. The actual end-tidal CO<sub>2</sub> is continuously sampled throughout the experiment to ensure targeted levels were indeed reached. The measured end-tidal CO<sub>2</sub> values are then used for calculations of CVR. The first targeted elevation of end-tidal CO<sub>2</sub> lasted for 45 seconds, followed by a return to baseline for 90 seconds, then a second increase lasted for 130 seconds followed by a return to baseline. For measurement of CVR, the second longer duration of hypercapnea is to allow for maximum response in pathologic areas that may be slow to respond. This resulted in near square wave transitions between the patient's end-tidal CO<sub>2</sub> baseline and elevations (baseline plus 10 mmHg), usually within 1–3 breaths, and sustained end-tidal gas levels.

### **Motor Task**

Patients were given instructions to perform a bilateral finger-tapping task for 3 minutes with 15-second on and off cycles. Patients practiced the task beforehand. Four patients were excluded from the study because they could not complete the motor task.

### **Data Processing**

Image analysis was performed using Analysis of Functional NeuroImages (AFNI) v. 2.0.<sup>9</sup> An AFNI algorithm was used to calculate head motion for each BOLD MRI acquisition. All patients had less than 1 voxel-width head motion during the CVR study. The BOLD MR signal was regressed against the acquired PETCO<sub>2</sub> data on a voxel-by-voxel basis. PETCO<sub>2</sub> measurements were time shifted to the point of maximal correlation with the mean BOLD signal of the entire brain. The purpose of this is to compensate for the transit time delay from pulmonary to cerebral circulation. CVR was calculated as percent change of the BOLD MR signal intensity per mmHg PETCO<sub>2</sub>. Previous work describes this quantitative technique in more detail.<sup>2,10–12</sup>

### **CVR Mapping**

CVR maps are generated by overlaying a color-coded map representing CVR over the anatomical images. Healthy blood vessels are able to dilate in response to rising pCO<sub>2</sub> to increase CBF, and thus CVR is positive (color-coded red to yellow on CVR maps). CVR can also be negative in areas where there is reduced CBF in response to rising pCO<sub>2</sub> due to steal physiology (color-coded light blue to dark blue on CVR maps). Also, the CVR maps were thresholded using the associated correlation coefficient of the regression. Any voxels whose correlation coefficient falls between  $-0.125$  and  $+0.125$  are not displayed (colorless on CVR maps).

### **BOLD fMRI Response to Motor Task**

The localization of the motor cortex for the hand was described by Yousri et al.<sup>13</sup> The region of interest (ROI) for the right and left hands were drawn on the anatomical images, giving two ROIs for each patient. The ROI were verified by a neuroradiologist. The anatomical images were then automatically segmented into gray matter and white matter by the program SPM8 (Wellcome Department, University College London, UK) using the segment function to calculate tissue probability maps. A threshold of 0.7 was used to create the gray matter mask and the segmentations were checked visually for gross errors. Only the gray matter within the ROI was used for further analysis. Spatial smoothing was not performed for CVR calculations. A 5-mm full-width half-max Gaussian blurring kernel was applied using AFNI to smooth the BOLD fMRI dataset for calculation of BOLD fMRI responses to the motor task. The percent BOLD signal change between on and off cycles of finger-tapping was calculated and was compared with the CVR values for the same area.

### **Results**

Eleven patients with steno-occlusive disease and unilateral hemodynamic impairment were selected for this study. Patient demographics are listed in Table 1. A summary of the raw data for CVR and BOLD fMRI responses for all patients is shown in Table 2. Data is shown for a representative patient (#6) in Fig. 1. Data for other patients can be found in Supplemental Fig. 1. The left panel shows the anatomical image that was used to draw the region of interest around the motor cortex for the hand, and the gray matter within the motor cortex was used for further analysis. Arrows point to the area of the motor cortex for the hand. The corresponding CVR plot is shown in the center panel. This patient has impaired CVR in the left hemisphere (blue), and relatively normal CVR elsewhere (yellow and red). The activation map for the finger-tapping motor task is shown for the same patient in the right panel. High levels of activation can be seen in the right hemisphere surrounding the motor cortex (yellow), but activation is not seen in the left hemisphere.

The average BOLD fMRI response to the finger-tapping motor task within each ROI during the on-off cycles of the motor task for Patient 11 is shown in Fig. 2. The ROI in the left hemisphere where there was positive CVR shows activation that follows the motor task, but in the right hemisphere where there was poor CVR, there is little activation that follows the on-and-off task cycles. The distribution of CVR versus BOLD fMRI for each voxel within each of the ROIs from Patient 11 is shown in Fig. 3. Voxels from the right hemisphere with negative CVR are color-coded blue, and show very low levels of activation on fMRI in response to the motor task. Voxels from the left hemisphere with positive CVR are color-coded red, and show higher levels of activation on fMRI in response to the motor task.

**TABLE 2. Patient Demographics and Correlation Statistics**

Subjects	Left hemisphere					Right hemisphere				
	Mean GM CVR (SD) [% ΔBOLD/ mmHg]	Mean BOLD fMRI response [% ΔBOLD]	R <sup>2</sup> of correlation	Size of ROI [mm <sup>3</sup> ]	# of EPI voxels included in ROI [voxels]	Mean GM CVR (SD) [% ΔBOLD/ mmHg]	Mean BOLD fMRI response [% ΔBOLD]	R <sup>2</sup> of correlation	Size of ROI [mm <sup>3</sup> ]	# of EPI voxels included in ROI [voxels]
1	0.17 (0.40)	0.40 (0.60)	0.54	1049	37	0.11 (0.08)	0.61 (0.39)	$7.5 \times 10^{-2}$	1186	45
2	0.02 (0.03)	-0.10 (0.27)	0.17	843	26	0.01 (0.03)	-0.22 (0.37)	0.14	948	23
3	-0.09 (0.06)	-0.08 (0.17)	0.02	898	60	0.09 (0.07)	0.33 (0.33)	0.27	1043	58
4	0.12 (0.11)	1.03 (0.46)	0.58	1365	39	0.12 (0.07)	0.62 (0.61)	0.01	1480	45
5	-0.02 (0.10)	-0.26 (0.17)	0.11	1079	37	0.04 (0.10)	0.03 (0.09)	$4.4 \times 10^{-2}$	378	26
6	-0.06 (0.11)	-0.08 (0.12)	0.07	1009	28	0.22 (0.08)	0.88 (0.43)	0.06	563	24
7	0.21 (0.09)	0.63 (0.83)	0.05	1178	31	0.15 (0.08)	0.76 (0.72)	0.11	852	41
8	0.13 (0.11)	0.78 (0.95)	0.25	1136	39	0.87 (0.14)	0.24 (0.15)	0.08	1199	36
9	0.04 (0.07)	-0.04 (0.07)	0.08	1349	57	-0.03 (0.06)	0.03 (0.09)	0.09	1110	54
10	0.14 (0.07)	0.79 (0.56)	0.02	524	33	$5.01 \times 10^{-3}$	-0.10 (0.45)	0.07	494	24
11	0.11 (0.11)	0.98 (0.87)	0.34	877	45	-0.05 (0.09)	0.06 (0.15)	0.13	1135	30

Voxels used for the calculation of BOLD fMRI were included in ROIs only if they had a 70% gray matter probability. CVR = cerebrovascular reactivity; GM = gray matter; ROI = region of interest (ROI was drawn over the hand representation of the motor cortex on T1-weighted images); SD = standard deviation.

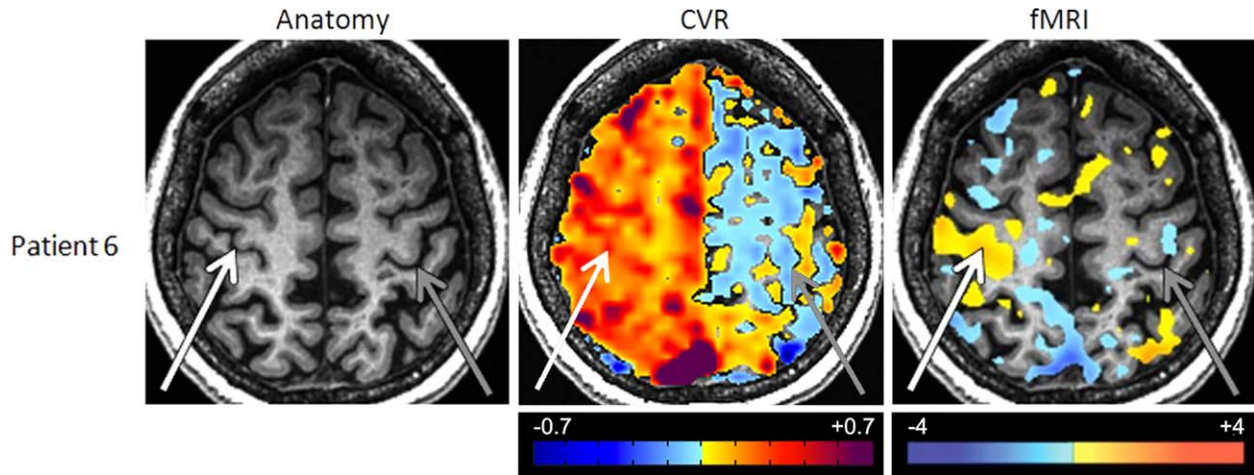


FIGURE 1: Comparison between anatomical, CVR, and fMRI maps in subject with unilateral carotid occlusion (Patient 6).

The average BOLD fMRI response to the finger-tapping motor task of each ROI of the 11 patients versus average CVR is shown in Fig. 4. Neuronal activation from the motor task was found to be linearly correlated with CVR (11 patients, 22 ROIs,  $R = 0.82$ ). Regions with positive (normal) CVR showed positive neuronal activation, while regions with negative CVR had attenuated neuronal activation on fMRI.

**Discussion**

This study quantitatively characterized the relationship between CVR and BOLD fMRI responses, a relationship that appears linear in regions with positive gray matter CVR. Assessing CVR is critical when applying BOLD imaging for clinical use and should be used to identify the regions where BOLD signal is detectable. Cerebrovascular disease affects coupling between neuronal activity and cerebral blood flow, and this study demonstrates that CVR mapping can predict areas where measurement of traditional

BOLD fMRI studies will be inaccurate. Our findings show that it is very important not to interpret the regions where there is no BOLD signal change due to impaired CVR. This has important implications for all studies that use BOLD fMRI as a measure of neuronal activation.

Figure 4 shows 10 data points that have a CVR below 0.05% BOLD/mmHg with either blunted or negative BOLD fMRI responses to the motor task. These data points arise from the hemisphere with impaired CVR in patients (Patients 3, 6, and 10) or from patients with bilateral stenotic-occlusive disease (Patients 2, 3, 5, and 9), all of which also had impaired CVR. This result suggests that a critical threshold for significantly impaired CVR exists at 0.05% BOLD/mmHg.

This study raises concerns over fMRI studies that have been performed in patients with ischemic stroke. Since a high percentage of these patients would have presented with significant stenotic-occlusive disease as a source of their

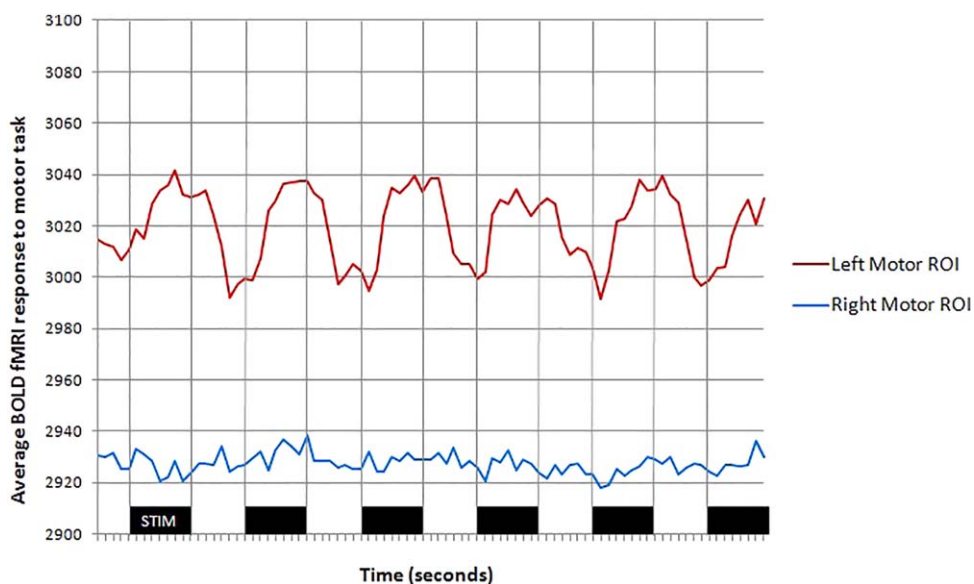


FIGURE 2: Average BOLD fMRI response within each ROI during the on-off cycles of the motor task (Patient 11).

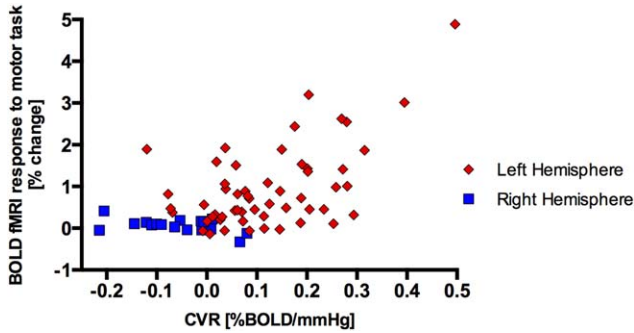


FIGURE 3: Average BOLD fMRI response versus CVR within each voxel (Patient 11).

ischemic event, lack of pretesting with CVR investigation to validate the BOLD response raises serious questions about the validity of the reported results. This cautionary observation also pertains to the use of BOLD fMRI for presurgical mapping in patients at risk for exhausted vascular reserve in whom normal cerebral cortex near or being infiltrated by tumor is being investigated.

Several studies have also investigated the effect of cerebrovascular disease on BOLD fMRI response and observed a decrease in the BOLD signal in patients with areas of impaired vasodilatory capacity due to steno-occlusive disease,<sup>14–16</sup> stroke,<sup>17–20</sup> and brain tumours.<sup>21,22</sup> These studies assessed the burden of cerebrovascular disease by multiple methods (transcranial Doppler ultrasonography, BOLD MRI CVR mapping, or single-photon emission computed tomography) using various vasodilatory stimuli (acetazolamide, CO<sub>2</sub>, hyperventilation, or breath-hold), so direct comparison is difficult. However, they similarly showed that diseased areas had reduced activation on traditional BOLD fMRI. Interestingly, fMRI in a moyamoya subject during a finger-tapping task reported cortical and cerebellar activation interpreted as reorganization following revascularization.<sup>23</sup> However, the observations that were made raise questions as

to whether fMRI findings under these circumstances represent true network reorganization as opposed to BOLD signal changes developing secondary to improved neurovascular coupling in the absence of network reorganization. Magnetoencephalography might prove beneficial in sorting this out. The issue is further complicated by the effect of selection of thresholds for displaying fMRI data. Figure 1 and Supplemental Fig. 1 refer to fMRI maps that are visually thresholded at a correlation of 0.3, a level lower than is typically applied for generating activation maps. Not surprisingly, this results in activation through much of the brain. Nevertheless, it is possible for a bilateral finger-tapping task to engage areas in the primary motor cortex, supplementary motor area, cingulate motor area, premotor area, frontal operculum, cerebellum, and somatosensory cortex.<sup>24</sup>

The reduction in BOLD signal changes seen in this study may be due to a number of factors, including a reduction in the speed of the vascular response,<sup>12</sup> or a temporal lag in the hemodynamic response function (HRF).<sup>25</sup> In patients with steno-occlusive and moyamoya disease, the HRF is known to differ from the canonical fMRI HRF, involving changes in the magnitude of the BOLD response and time delay, shown in resting-state fMRI studies.<sup>26–28</sup> Although it may be possible that the negative BOLD signal may in actuality be representative of a positive result with a delay such that it appears out of phase with the finger-tapping task, this is highly unlikely. We have previously shown that the temporal delay in areas of negative BOLD signal in response to a 10-mmHg hypercapnic step change in PETCO<sub>2</sub> was in the range of 0–3 seconds.<sup>25</sup>

It is not possible to assess the functional level of tissue with impaired CVR, not because it is not functioning but because its response to any vasodilatory stimulus is unknown.<sup>2,22</sup> Indeed, one study also compared neuronal

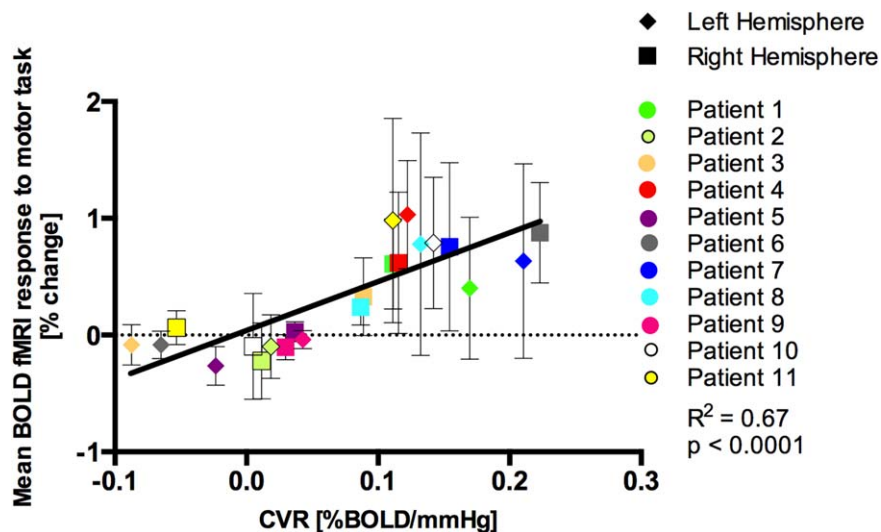


FIGURE 4: Average BOLD fMRI response to the finger-tapping motor task versus CVR within each ROI of all 11 patients.

activation as measured with magnetoencephalographic (MEG)-evoked fields compared to BOLD fMRI and demonstrated neuronal activity observed with MEG that was not observed on fMRI.<sup>16</sup> This further supports the observation that there will be areas of reduced activation on BOLD fMRI when there is cerebrovascular disease sufficient to reduce CVR. Thus, an understanding of the vasoreactive status of patients' brains is necessary when interpreting functional imaging results.

This study demonstrates a parametric relationship between CVR and fMRI task activation in that the degree of impairment in CVR is directly related to the loss of signal on traditional BOLD fMRI. This was a somewhat surprising result in view of the nonlinearities inherent within the BOLD signal as a function of blood flow and task activation.

CVR mapping is clinically easy to implement alongside traditional BOLD fMRI studies. In this study we used a custom gas blender to administer CO<sub>2</sub>, and targeted an elevation in end-tidal PCO<sub>2</sub>. This system provides precise control and measurement of end-tidal PCO<sub>2</sub>. Other groups have performed CVR mapping using a breath-hold protocol where patients alternate normal periods of breathing with 10–30-second breath-holds to induce hypercapnia.<sup>22</sup> The advantage of this technique is that it requires no additional equipment; however, it may be limited by the patients' ability to cooperate with the protocol, thereby decreasing the reliability of the CVR measurement.

There are some limitations to this study. The study design used a bilateral finger-tapping task which may potentially confound the activation results on traditional BOLD fMRI. However, the patients selected for this study had steno-occlusive disease, resulting in decreased cerebral blood flow to one hemisphere, but had not experienced any major vascular event such as stroke. In addition, they had normal brain anatomical scans, and they did not have any motor deficits. In these patients we would not expect any remapping occur, such as that seen in some patients following major events such as stroke, that may cause confounding from crossed contralateral control. Another potential limitation of the study design was the choice of 15-second task blocks. In severely diseased areas of the brain it is possible that it may take longer than 15 seconds to observe a maximal response. However, other studies have observed maximal responses within less than 15 seconds.<sup>14,17</sup>

In conclusion, CVR mapping is a noninvasive MRI-based imaging technique that can provide information about the vascular reactivity of the brain that is necessary for validating BOLD fMRI responses and preventing false-negative type II errors in patients with disorders that could affect vascular reserve. In fact, further work may enable implementation of correction factors based on CVR responses to

“normalize” BOLD activation data in patients with cerebrovascular disease undergoing fMRI studies.

## Acknowledgments

This work was presented as a poster at RSNA in Chicago, November 30th, 2014. We thank the RespirAct technologist Anne Battisti-Charbonney and MR imaging technologists, Keith Ta and Eugen Hlasny.

## Conflict of Interest

AEP and KS have no conflicts of interest to declare. JAF, JP, APC, DJM contributed to the development of the RespirAct and have an interest in Thornhill Research Inc., a spin-off company of the University Health Network where they are employed or have practice privileges. The RespirAct is not a commercial product and was made available for this project by TRI. TRI did not otherwise review the data or the article.

## References

1. Attwell D, Buchan AM, Charpak S, et al. Glial and neuronal control of brain blood flow. *Nature* 2010;468:232–243.
2. Sobczyk O, Battisti-Charbonney A, Fierstra J, et al. A conceptual model for CO<sub>2</sub>-induced redistribution of cerebral blood flow with experimental confirmation using BOLD MRI. *Neuroimage* 2014;92:56–68.
3. Davis TL, Kwong KK, Weisskoff RM, Rosen BR. Calibrated functional MRI: mapping the dynamics of oxidative metabolism. *Proc Natl Acad Sci U S A* 1998;95:1834–1839.
4. Mandell DM, Han JS, Poublanc J, et al. Mapping cerebrovascular reactivity using blood oxygen level-dependent MRI in Patients with arterial steno-occlusive disease: comparison with arterial spin labeling MRI. *Stroke* 2008;39:2021–2028.
5. Fierstra J, Poublanc J, Han JS, et al. Steal physiology is spatially associated with cortical thinning. *J Neurol Neurosurg Psychiatry* 2010;81:290–293.
6. Slessarev M, Han J, Mardimae A, et al. Prospective targeting and control of end-tidal CO<sub>2</sub> and O<sub>2</sub> concentrations. *J Physiol* 2007;581(Pt 3):1207–1219.
7. Prisman E, Slessarev M, Han J, et al. Comparison of the effects of independently-controlled end-tidal PCO<sub>2</sub> and PO<sub>2</sub> on blood oxygen level-dependent (BOLD) MRI. *J Magn Reson Imaging* 2008;27:185–191.
8. Ito S, Mardimae A, Han J, et al. Non-invasive prospective targeting of arterial P(CO<sub>2</sub>) in subjects at rest. *J Physiol* 2008;586(Pt 15):3675–3682.
9. Cox RW. AFNI: software for analysis and visualization of functional magnetic resonance neuroimages. *Comput Biomed Res* 1996;29:162–173.
10. Sobczyk O, Crawley AP, Poublanc J, et al. Identifying significant changes in cerebrovascular reactivity to carbon dioxide. *AJNR Am J Neuroradiol* 2016;37:818–824.
11. Sobczyk O, Battisti-Charbonney A, Poublanc J, et al. Assessing cerebrovascular reactivity abnormality by comparison to a reference atlas. *J Cereb Blood Flow Metab* 2015;35:213–220.
12. Poublanc J, Crawley AP, Sobczyk O, et al. Measuring cerebrovascular reactivity: the dynamic response to a step hypercapnic stimulus. *J Cereb Blood Flow Metab* 2015;35:1746–1756.
13. Yousry TA, Schmid UD, Alkadhi H, et al. Localization of the motor hand area to a knob on the precentral gyrus. A new landmark. *Brain* 1997;120(Pt 1):141–157.

14. Carusone LM, Srinivasan J, Gitelman DR, Mesulam MM, Parrish TB. Hemodynamic response changes in cerebrovascular disease: implications for functional MR imaging. *AJNR Am J Neuroradiol* 2002;23:1222–1228.
15. Siero JC, Hartkamp NS, Donahue MJ, et al. Neuronal activation induced BOLD and CBF responses upon acetazolamide administration in patients with steno-occlusive artery disease. *Neuroimage* 2015;105:276–285.
16. Rossini PM, Altamura C, Ferretti A, et al. Does cerebrovascular disease affect the coupling between neuronal activity and local haemodynamics? *Brain* 2004;127(Pt 1):99–110.
17. Hamzei F, Knab R, Weiller C, Rother J. The influence of extra- and intracranial artery disease on the BOLD signal in fMRI. *Neuroimage* 2003;20:1393–1399.
18. Krainik A, Hund-Georgiadis M, Zysset S, von Cramon DY. Regional impairment of cerebrovascular reactivity and BOLD signal in adults after stroke. *Stroke* 2005;36:1146–1152.
19. Murata Y, Sakatani K, Hoshino T, et al. Effects of cerebral ischemia on evoked cerebral blood oxygenation responses and BOLD contrast functional MRI in stroke patients. *Stroke* 2006;37:2514–2520.
20. Sakatani K, Murata Y, Fujiwara N, et al. Comparison of blood-oxygen-level-dependent functional magnetic resonance imaging and near-infrared spectroscopy recording during functional brain activation in patients with stroke and brain tumors. *J Biomed Opt* 2007;12:062110.
21. Pillai JJ, Zaca D. Clinical utility of cerebrovascular reactivity mapping in patients with low grade gliomas. *World J Clin Oncol* 2011;2:397–403.
22. Pillai JJ, Mikulis DJ. Cerebrovascular reactivity mapping: an evolving standard for clinical functional imaging. *AJNR Am J Neuroradiol* 2015;36:7–13.
23. Calabro RS, Bramanti P, Baglieri A, et al. Functional cortical and cerebellar reorganization in a case of moyamoya disease. *Innov Clin Neurosci* 2015;12:24–28.
24. Small SL, Hlustik P, Noll DC, Genovese C, Solodkin A. Cerebellar hemispheric activation ipsilateral to the paretic hand correlates with functional recovery after stroke. *Brain* 2002;125(Pt 7):1544–1557.
25. Poublanc J, Han JS, Mandell DM, et al. Vascular steal explains early paradoxical blood oxygen level-dependent cerebrovascular response in brain regions with delayed arterial transit times. *Cerebrovasc Dis Extra* 2013;3:55–64.
26. Lv Y, Margulies DS, Cameron Craddock R, et al. Identifying the perfusion deficit in acute stroke with resting-state functional magnetic resonance imaging. *Ann Neurol* 2013;73:136–140.
27. Christen T, Jahanian H, Ni WW, et al. Noncontrast mapping of arterial delay and functional connectivity using resting-state functional MRI: a study in moyamoya patients. *J Magn Reson Imaging* 2015;41:424–430.
28. Amemiya S, Kunimatsu A, Saito N, Ohtomo K. Cerebral hemodynamic impairment: assessment with resting-state functional MR imaging. *Radiology* 2014;270:548–555.